

## Polymer Dielectric Films Exhibiting Superior High-Temperature Capacitive Performance by Utilizing an Inorganic Insulation Interlayer

Tiandong Zhang,<sup>a</sup> Lianyin Yang,<sup>a</sup> Changhai Zhang,<sup>a</sup> Yu Feng,<sup>a</sup> Jian Wang,<sup>b</sup> Zhonghui Shen,<sup>\*b</sup> Qingguo Chen,<sup>a</sup> Qingquan Lei,<sup>a</sup> Qingguo Chi,<sup>\*a</sup>

T. D. Zhang, L. Y. Yang, C. H. Zhang, Y. Feng, Q. G. Chi, Q. G. Chen, Q. Q. Lei

E-mail: [qgchi@hrbust.edu.cn](mailto:qgchi@hrbust.edu.cn)

<sup>a</sup>School of Electrical and Electronic Engineering

Harbin University of Science and Technology

Harbin, China

J. Wang, Z. H. Shen

E-mail: [zhshen@whut.edu.cn](mailto:zhshen@whut.edu.cn)

<sup>b</sup>International School of Materials Science and Engineering

Wuhan University of Technology

Wuhan, China

### Finite-element simulations

In order to qualitatively understand the charge carrier behaviors in nanocomposites, a unipolar electron injection and transport model is established. Here, we describe electrons injected from the metal electrode into the dielectric by Schottky thermionic emission, which is expressed as

$$J_e = AT^2 \exp\left(-\frac{\phi_i}{k_B T}\right) \exp\left(\frac{e}{k_B T} \sqrt{\frac{eE}{4\pi\epsilon_0\epsilon_r}}\right) \quad (\text{S1})$$

where  $J$  is the current density,  $A$  is the Richardson constant,  $T$  is the temperature,  $\phi_i$  is the injection potential barrier,  $k_B$  is the Boltzmann constant,  $e$  is the elementary charge,  $E$  is the electric field,  $\epsilon_0$  is the vacuum permittivity,  $\epsilon_r$  is the relative permittivity, respectively.

The behavior of charge within the films is governed by the following equations:

Poisson's equation,

$$\frac{\partial\psi(\mathbf{r}, t)}{\partial r_i \partial r_j} = \frac{\rho(\mathbf{r}, t)}{\epsilon_0 \epsilon_r} \quad (2)$$

Current continuity equation,

$$\frac{\partial n(\mathbf{r}, t)}{\partial t} + \frac{\partial J(\mathbf{r}, t)}{\partial r} = s \quad (3)$$

Charge transport equation,

$$J(r, t) = \mu(r, t)n(r, t)E(r, t) \quad (4)$$

where  $\psi$  the electrical potential,  $\rho$  the total charge density (here equal  $n(r, t)$ ),  $s$  the source term ( $s=0$  in this simulation),  $\mu$  the mobility of charge.

**Table 1**

Definition of parameters used in this simulation.

Parameter	Values	Units
Charge mobility of PEI	$1 \times 10^{-10}$	$\text{cm}^2/(\text{V}\cdot\text{s})$
Charge mobility of MgO	$1 \times 10^{-13}$	$\text{cm}^2/(\text{V}\cdot\text{s})$
Dielectric constant of PEI	3.15	---
Dielectric constant of MgO	9.8	---
Electric field	100	MV/m
Temperature	423	K
Schottky barrier	1.55	eV

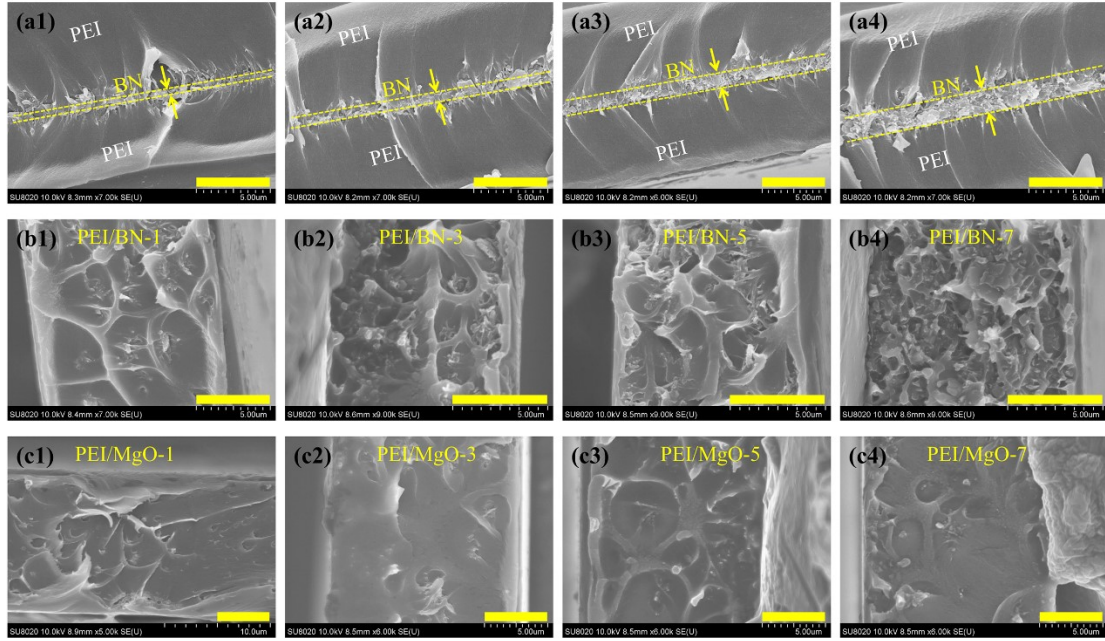


**Figure S1** Cross-sectional structure of SEM images of (a) PBP films. (b) PEI/BN films. (c) PEI/MgO films.

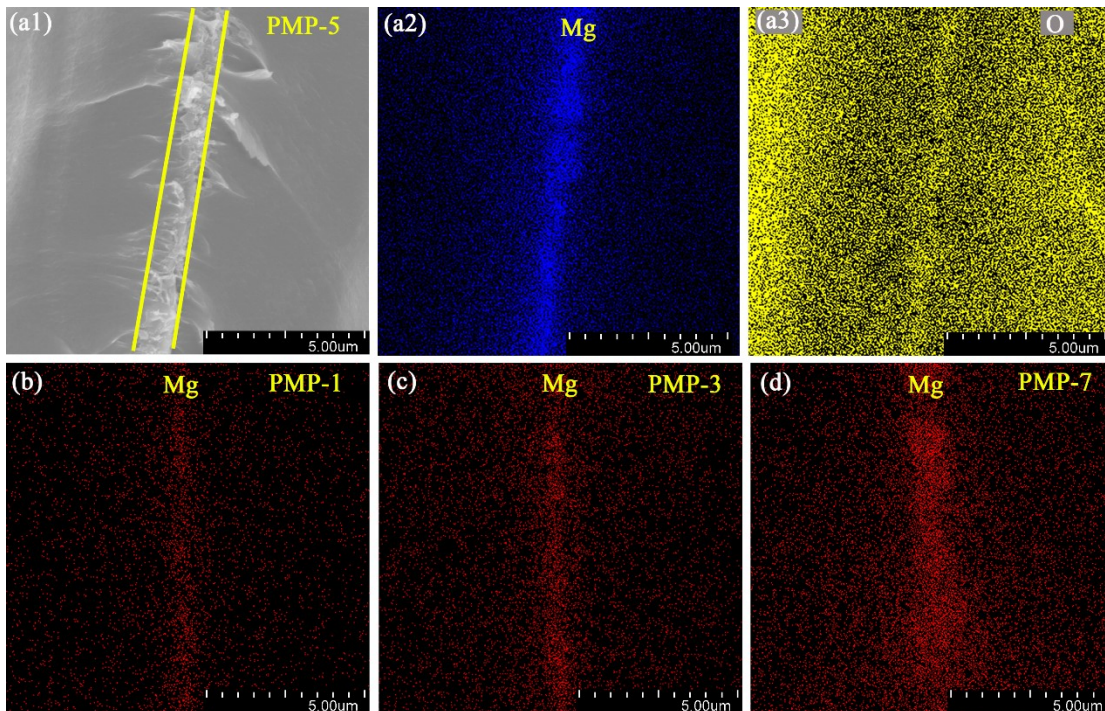


**Figure S2** SEM-EDX mapping of PMP films.

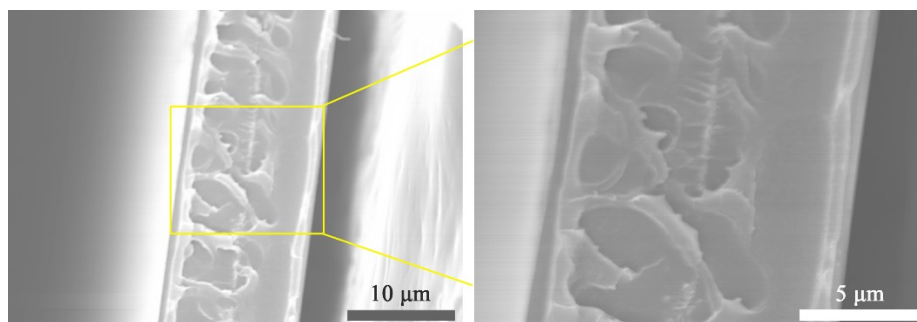


**Figure S3** Representative low-magnification of SEM image of PMP films.

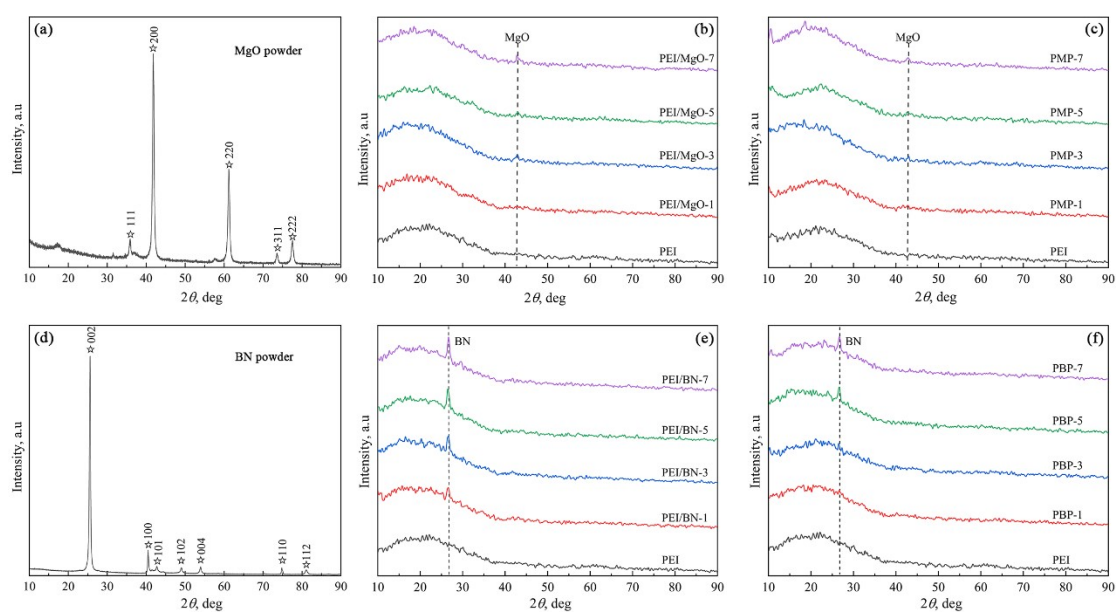


**Figure S4** XRD patterns of (a) MgO powder. (b) PEI/MgO films. (c) PMP films. (d) BN powder. (e) PEI/BN films. (f) PBP films.

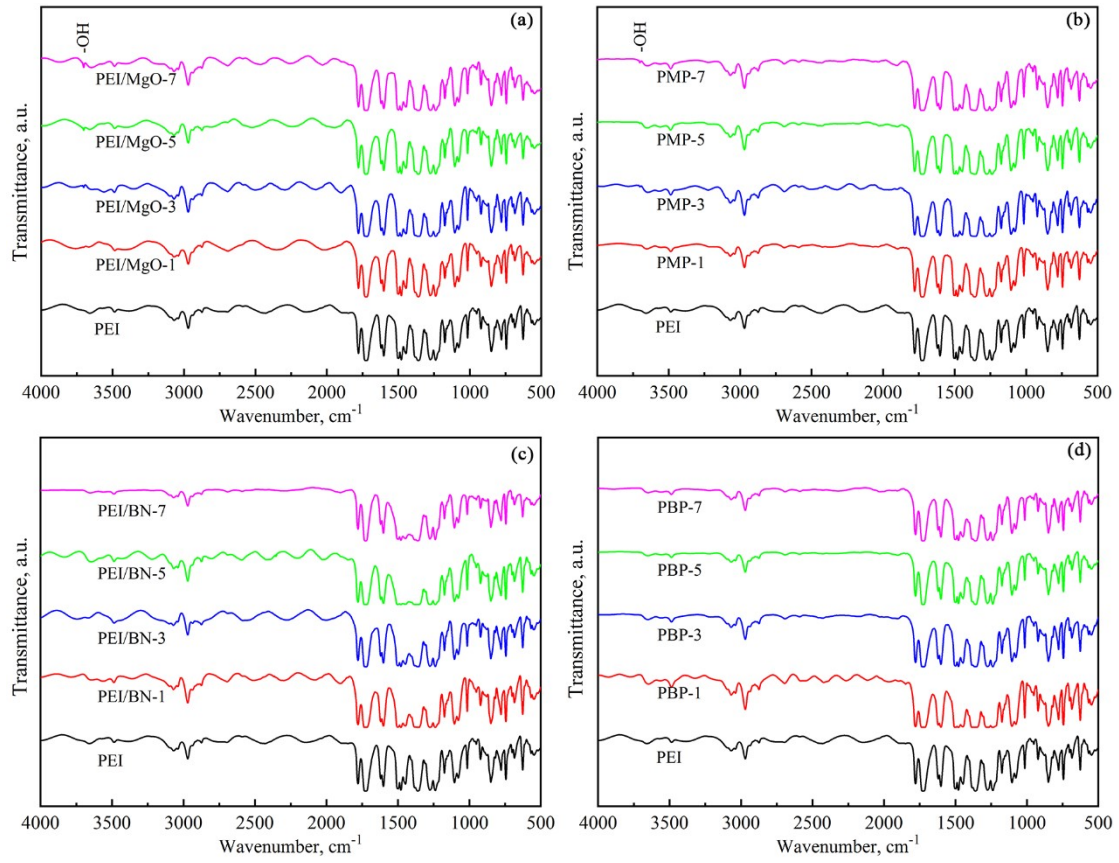


**Figure S5** FTIR spectra of (a) PEI/MgO films. (b) PMP films. (c) PEI/BN films. (d) PBP films.

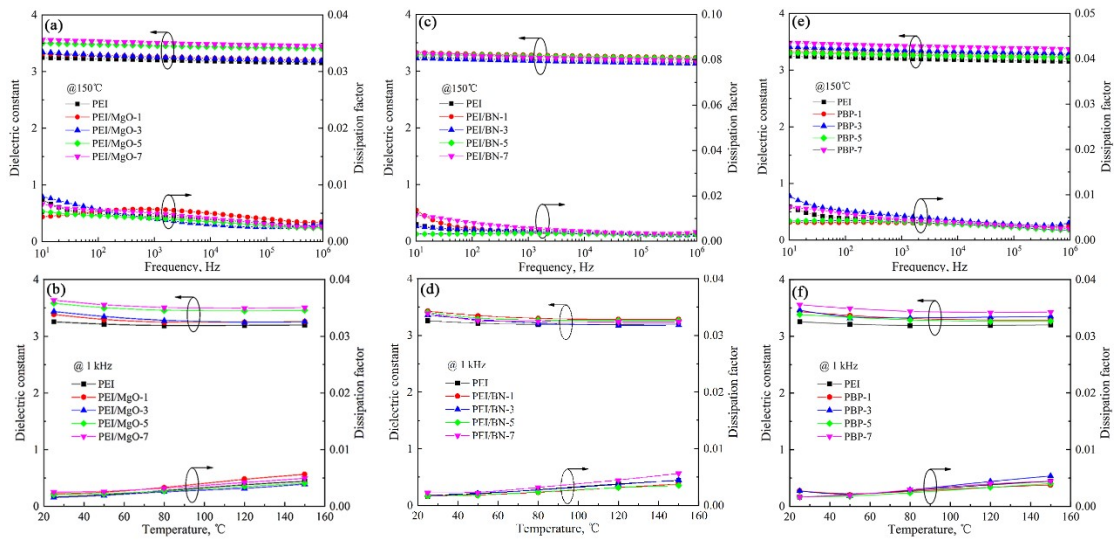


**Figure S6** Frequency-dependent and temperature-dependent dielectric properties measured at 150°C and 1 kHz, respectively. (a) (b) PEI/MgO films. (c) (d) PEI/BN films. (e) (f) PBP films.

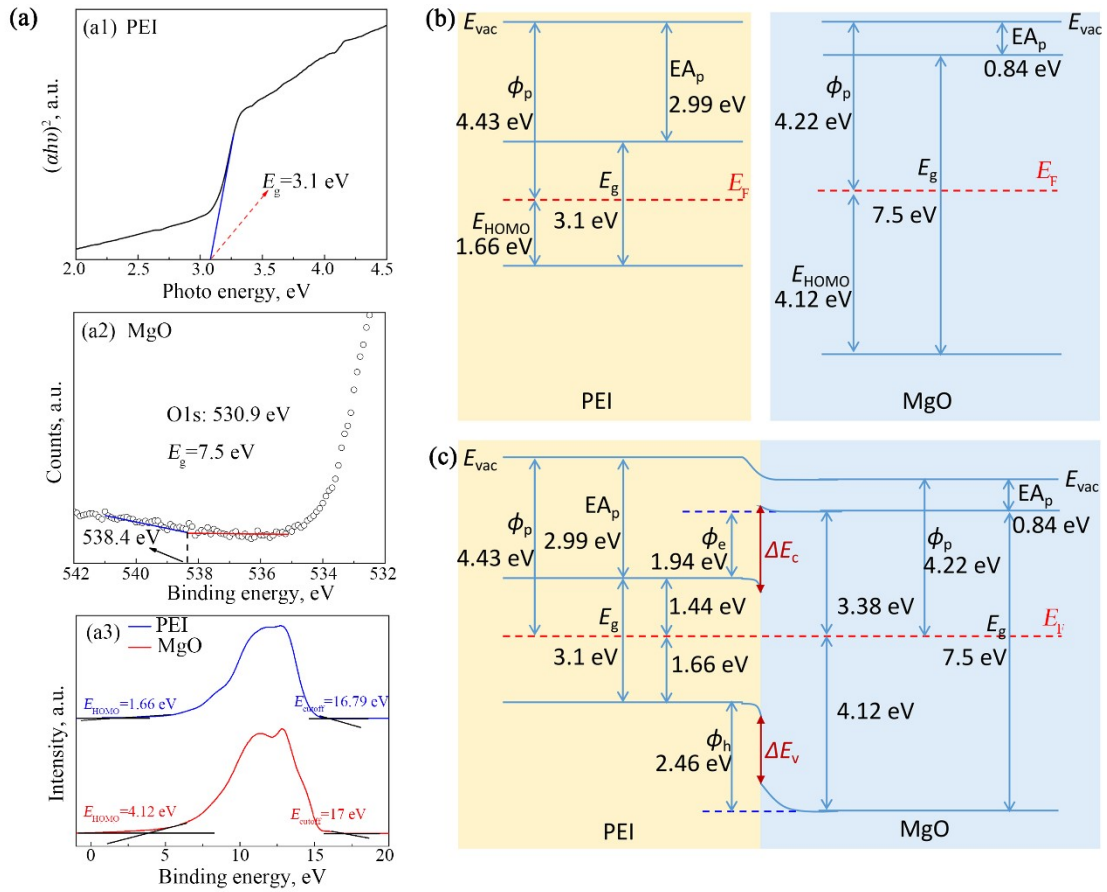


**Figure S7** Electronic structure of (a1) PEI, (a2) MgO, (a3) PEI and MgO. Band diagrams at PEI/MgO interface. (b) PEI and MgO interlayer before contact. (c) PEI and MgO interlayer after contact. Herein,  $E_g$  is bandgap,  $E_F$  is Fermi levels,  $E_{\text{HOMO}}$  stands for the highest occupied molecular orbital of the dielectric,  $E_{\text{cutoff}}$  represents the energy of secondary electron cutoff.  $\phi_p$  is the work function,  $E_{\text{vac}}$  is the vacuum energy level.  $\phi_e$  is the potential barrier for electrons, and  $\phi_h$  is the potential barrier for holes.

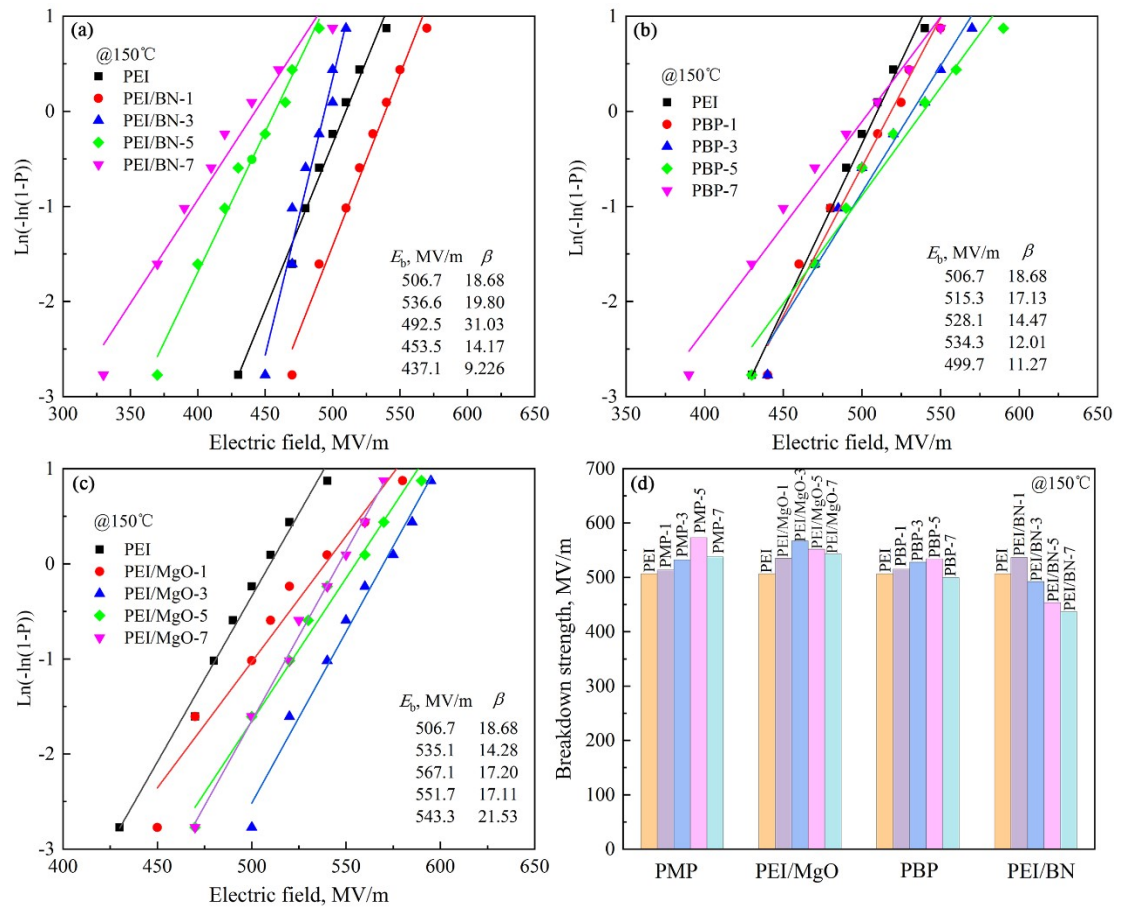


**Figure S8** Weibull distribution of (a) PEI/BN films. (b) PBP films. (c) PEI/MgO films measured at 150°C. (d) Comparison of breakdown strength of resultant films in this work measured at 150°C.

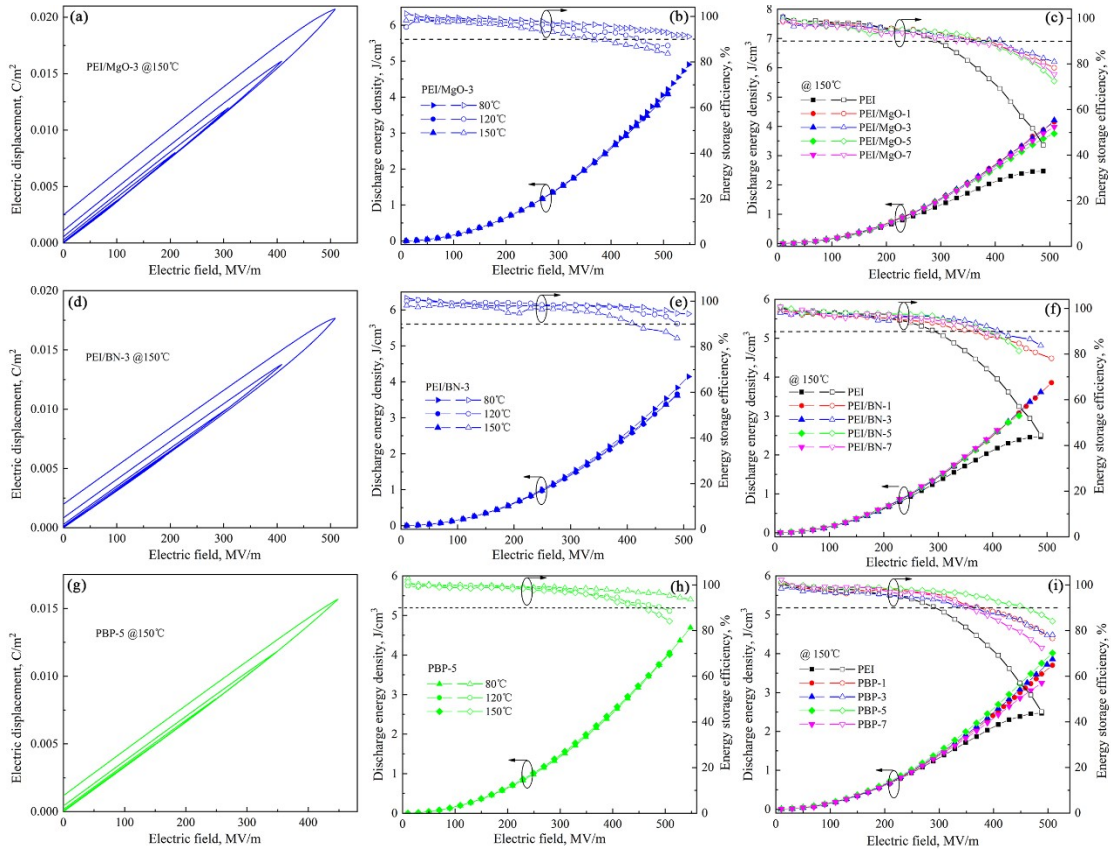


**Figure S9** Hysteresis loops measured at 150°C of (a) PEI/MgO-3 film. (d) PEI/BN-3 film. (g) PBP-5 film. Discharged energy density and efficiency of (b) PEI/MgO-3 film. (e) PEI/BN-3 film. (h) PBP-5 film at various temperatures. Discharged energy density and efficiency of (c) PEI/MgO films. (f) PEI/BN films. (i) PBP films measured at 150°C.

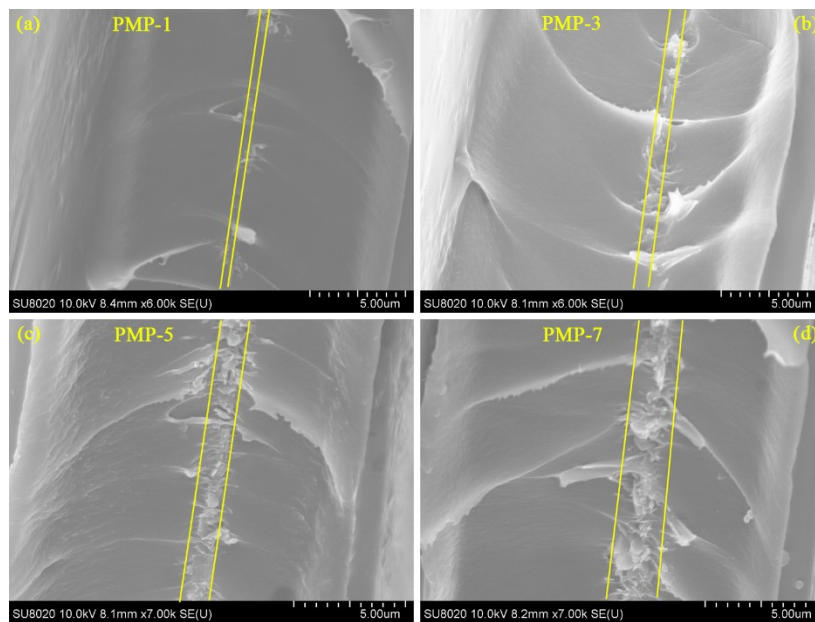


**Figure S10** Cross-sectional structure of SEM images of PMP films after 50000 charge/discharge cycles.